May, 1993

SEABED STABILITY MONITORING AT DUMP SITE B OF ST. JOHN HARBOUR, NEW BRUNSWICK, USING SEA CAROUSEL

prepared by

Carl. L. Amos(1), K-L. Tay(2), M. Hughes(1), A. Robertson(2) and B. Wile(1)

(1) Geological Survey of Canada
Bedford Institute of Oceanography
Dartmouth, Nova Scotia

(2) Marine Environment Branch, Environment Protection
Environment Canada, 45 Alderney Drive
Dartmouth, Nova Scotia, B2Y 2N6

(3) Eiger Enterprises
61 Laurie Street, Truro,
Nova Scotia, B2N 4S8

Internal Technical Report

1.0 EXECUTIVE SUMMARY

A series of 6 Sea Carousel deployments were undertaken at strategic sites near the mouth of St. John Harbour, New Brunswick to determine the stability of dredge spoil that had been dumped in previous years. The work was carried out aboard the vessel *Irish Lass* during 22nd and 23rd May, 1993. The period of the survey coincided with peak annual river discharge and consequently surface currents were at times in excess of 2 m/s. This conditions of flow lead to logistical difficulties in boat anchorage and Sea Carousel deployment. Also, current drag on the cables caused the Carousel to lift at times, and caused the umbilical to occasionally jam in the lid upon settlement of the Carousel. Nevertheless, 6 successful deployments were made from which several trends emerged relevant to seabed stability in the region. SJ1 and SJ2 were situated on the main 1992 dump site B. Surface currents here were in excess of 1 m/s. The seabed was composed of gravel and bedrock and was resistant to erosion by Sea Carousel. SJ3 and SJ4 were in deeper water adjacent to the main dump site and were composed of soft muddy sediments. These sediments showed a cohesion of *circa* 1.0 Pa and were both in a fluidized state (susceptible to liquefaction). SJ3 showed a reversal in strength with depth, being stronger at the surface than at depth. SJ5 was abandoned due to consistent loss of anchorage. SJ6 and SJ7 were situated on the reference site in St John Harbour. This site possessed a surface cohesive strength of 1.0 Pa and showed an increase in strength with depth - a profile typical of consolidating sediments.

Settling experiments were carried out at stations SJ3 and SJ6. Both exhibited a smooth exponential dec[illegible] suspended sediment concentration with a concentration half-life of *circa* 250 and 350 seconds respectively.

Types I and II erosion were detected; Type II erosion dominated the experiments suggestive of a chronic erosion potential for the fine-grained sites (SJ3, SJ4, SJ6 and SJ7). The erosion rates detected at site SJ3 were the highest ever recorded by the Sea Carousel for both Types of erosion, and attest to the potential for resuspension. The surface cohesion values were typical of newly-deposited muds. The transition from seabed erosion and armouring to one of deposition took place between the depths of 12 and 19 m. Above 12 m the seabed is scoured by natural processes; below 19 m deposition of fines predominates under natural conditions. Stations SJ1 and SJ2 fall into the shallow, armoured region, while stations SJ3, SJ4, SJ6 and SJ7 fall into the deeper, depositional region.

2.0 LIST OF CONTENTS

3.0 LIST OF FIGURES

change in sediment strength with depth in the sediment. The cohesion is in excess of our applied stress and the friction angle is 90°.

FIGURE 6.2.3. A time-series plot of measurements made at station SJ2 (1992 dump site B) for the period 16.8 to 17.6 (GMT) 22 May, 1993. The figure shows: (A) lid rotation, azimuthal current speed, and vertical current speed (m/s); (B) the corrected suspended sediment concentration (mg/L) for OBS1 (lower), OBS2 (ambient) and OBS3 (upper). Also shown is the raw mean carousel SSC (uncorrected for dispersion); and (C) the erosion rate ($kg/m^2/s$) based on the rate of change in SSC within the Carousel.

FIGURE 6.2.4. The applied bed shear stress plotted against the depth eroded during the Sea Carousel experiment SJ2. Also shown is the effective stress. The slope of the line is proportional to the friction angle and the intercept is a measure of cohesion (or the critical bed shear stress of surface erosion). The cluster of points map the change in sediment strength with depth in the sediment. The cohesion is 0.5 Pa and the friction angle is 87°.

FIGURE 6.2.5. A time-series plot of measurements made at station SJ3 (west of 1992 dump site B) for the period 19.3 to 20.4 (GMT) 22 May, 1993. The figure shows: (A) lid rotation, azimuthal current speed, and vertical current speed (m/s); (B) the corrected suspended sediment concentration (mg/L) for OBS1 (lower), OBS2 (ambient) and OBS3 (upper). Also shown is the raw mean carousel SSC (uncorrected for dispersion); and (C) the erosion rate ($kg/m^2/s$) based on the rate of change in SSC within the Carousel.

FIGURE 6.2.6. The applied bed shear stress plotted against the depth eroded during the Sea Carousel experiment SJ3. Also shown is the effective stress. The slope of the line is proportional to the friction angle and the intercept is a measure of cohesion (or the critical bed shear stress

of surface erosion). The cluster of points map the change in sediment strength with depth in the sediment. The cohesion is 1.0 Pa and the friction angle is 0° (fluidized bed).

FIGURE 6.2.7. The raw suspended sediment concentration within the Sea Carousel plotted against time during the still-water settling experiment carried out at the termination of station SJ3. Notice the steady exponential decay in concentration with an approximate half-life of 360 seconds.

FIGURE 6.2.8. A time-series plot of measurements made at station SJ4 (west of 1992 dump site) for the period 22.0 to 23.2 (GMT) 22 May, 1993. The figure shows: (A) lid rotation, azimuthal current speed, and vertical current speed (m/s); (B) the corrected suspended sediment concentration (mg/L) for OBS1 (lower), OBS2 (ambient) and OBS3 (upper). Also shown is the raw mean carousel SSC (uncorrected for dispersion); and (C) the erosion rate ($kg/m^2/s$) based on the rate of change in SSC within the Carousel.

FIGURE 6.2.9. The applied bed shear stress plotted against the depth eroded during the Sea Carousel experiment SJ4. Also shown is the effective stress. The slope of the line is proportional to the friction angle and the intercept is a measure of cohesion (or the critical bed shear stress of surface erosion). The cluster of points map the change in sediment strength with depth in the sediment. The cohesion is 1.0 Pa and the friction angle is 0° (fluidized bed).

FIGURE 6.2.10. A time-series plot of measurements made at station SJ6 (the reference site) for the period 13.4 to 14.9 (GMT) 23 May, 1993. The figure shows: (A) lid rotation, azimuthal current speed, and vertical current speed (m/s); (B) the corrected suspended sediment concentration (mg/L) for OBS1 (lower), OBS2 (ambient) and OBS3 (upper). Also shown is the raw mean carousel SSC (uncorrected for dispersion); and (C) the erosion rate ($kg/m^2/s$) based on

the rate of change in SSC within the Carousel.

FIGURE 6.2.11. The applied bed shear stress plotted against the depth eroded during the Sea Carousel experiment SJ6. Also shown is the effective stress. The slope of the line is proportional to the friction angle and the intercept is a measure of cohesion (or the critical bed shear stress of surface erosion). The cluster of points map the change in sediment strength with depth in the sediment. The cohesion is 1.0 Pa and the friction angle is 0° (fluidized bed).

FIGURE 6.2.12. The raw suspended sediment concentration within the Sea Carousel plotted against time during the still-water settling experiment carried out at the termination of station SJ3. Notice the steady exponential decay in concentration with an approximate half-life of 360 seconds.

FIGURE 6.2.13. A time-series plot of measurements made at station SJ7 (the reference site) for the period 15.0 to 16.2 (GMT) 23 May, 1993. The figure shows: (A) lid rotation, azimuthal current speed, and vertical current speed (m/s); (B) the corrected suspended sediment concentration (mg/L) for OBS1 (lower), OBS2 (ambient) and OBS3 (upper). Also shown is the raw mean carousel SSC (uncorrected for dispersion); and (C) the erosion rate ($kg/m^2/s$) based on the rate of change in SSC within the Carousel.

FIGURE 6.2.14. The applied bed shear stress plotted against the depth eroded during the Sea Carousel experiment SJ7. Also shown is the effective stress (depth x buoyant bulk weight). The slope of the line is proportional to the friction angle and the intercept is a measure of cohesion (or the critical bed shear stress of surface erosion). The cluster of points map the change in sediment strength with depth in the sediment. The cohesion is 1.0 Pa and the friction angle is 80°.

FIGURE 6.4.1. A scatter gram of peak erosion rate ($kg/m^2/s$) plotted against the excess bed shear

stress (Pa). A reasonable correlation exists between the two variable; the greater the excess shear stress, the higher the erosion rate.

4.0 THE SEA CAROUSEL

Sea Carousel, named after the carousels of Postma (1967) and Hydraulic Research Limited (Burt, 1984), is a benthic annular flume designed for field use in intertidal and subtidal settings. The carousel is 1.0 m in radius with an annulus 0.15 m wide and 0.30 m high (Figure 4.1). It weighs approximately 150 kg in air and 40 kg in water and is made entirely of aluminium. Flow in the annulus is induced by rotating a movable lid that is driven by a 0.35 hp DC motor powered from the surface. Eight small paddles, spaced equidistantly beneath the lid, induce a flow of water in the annulus. The width of the annulus (D) was made 0.15 m to give a relative roughness (e/D) $\approx$ 0.004 (where the wall roughness, e $\approx$ 0.0006 m; after Shames, 1962). The water depth in the annulus was minimized to 0.25 m to ensure conditions for Nikuradse's "rough-pipe zone of flow" wherein changes in wall friction factor with changes in Reynolds number are at a minimum (Shames, 1962).

A schematic diagram of the Sea Carousel configuration is shown in Figure 4.2. It is equipped with three optical backscatter sensors (OBS's; Downing, 1983). Two of these are located non-intrusively on the inner wall of the annulus at heights of 0.03 and 0.18 m above the skirt (the skirt is a horizontal flange situated around the outer wall of the annulus 0.04 m above the base; it was designed to standardize penetration of the flume into the seabed; see Figure 4.1). The third OBS detects ambient particle concentration outside the annulus, or it may be used to detect internal sediment concentration at a height between the other two. The OBS sensors give linear responses to particle concentration (of a constant size) for both mud and sand over a

concentration range of 0.1 to 50 g/L (Downing and Beach, 1989). They are unaffected by flows below 1.5 m/s and are stable through time. A sampling port is situated in the outer wall of the annulus at a height of 0.2 m above the skirt through which water samples can be drawn to calibrate the three sensors under well mixed conditions.

A Marsh/McBirney current meter (model 511) is located on the centreline of the annulus at a height of 0.16 m above the skirt. It was used to detect the instantaneous azimuthal and vertical components of flow within the annulus (U_y and U_w respectively). Mean tangential lid rotational speed ($\bar{U}_r$) is detected through a shaft end-coder resting on the lid. Controller boards for each sensor and the necessary power (12 VDC) are derived from an underwater pod located above the annulus. Output voltages from all sensors are digitized and transformed to scientific units on a Campbell Scientific CR10 data logger and stored on a Campbell Scientific SM192 storage module (storage capacity of 96,000 data values), also located in the underwater pod. The data logger is interrogated and programmed from the surface using a microcomputer linked to the data logger through an RS232 interface. Maximum sampling rate of all channels is approximately 2 Hz, whereas U_y and U_w may be logged at rates up to 10.66 Hz. All channels may be monitored and displayed on the surface computer allowing the operator to control the experiment interactively. Bed shear stress is varied in time by varying the power supplied to the underwater motor up to 350 watts via a surface power supply. The data stored from each deployment may be downloaded remotely through the RS232 cable at the end of each experiment and the storage module re-initialized.

A window is located in the inner flume wall for purposes of observing and recording the mechanics of bed failure. A perspex wedge at the base of the window sections the sediment upon

deployment. Thus the upper 20 mm of sediment and the lower 10 cm of the water column can be viewed in section. Visual observations are made using a Sony Handycam 8 mm video recorder model CCD-V11 held in an Amphibico Amphibian V11 underwater housing. Light is provided by two 100 watt underwater lights powered from the surface. The housing has a lens that corrects for underwater geometric distortions and so is suitable for accurate image scaling. The camera lens is located approximately 0.2 m from the window. Horizontal and vertical scale lines are present on the window and situated within the field of view. The camera images 100 frames/s. A co-axial cable connects the camera to a surface monitor for real-time detection. Video records are stored on a standard VHS video cassette recorder also at the surface. Sequential video images are digitized for particle trajectories at varying heights above the bed. From these, velocity profiles are constructed. From such profiles, thicknesses of the logarithmic part of the benthic boundary layer are determined and friction velocities computed. These latter values were then compared with laboratory measures.

Dispersion of suspended sediment out of the rotating annulus was observed on the video to take place during submerged deployments of Sea Carousel. Dispersion results from exchanges of water mass between the annulus (at concentration S_1) and the open marine environment (at concentration S_o) where $S_1 = S_o$. The rate of diffusion of mass (M) may be defined per unit cross-section area as:

$$\partial M/\partial t = - \delta \, \partial S/\partial x \qquad (1)$$

where δ is the coefficient of diffusivity (L^2T^{-1}) and x is a typical horizontal length scale, which in our case is unknown. Similarly, the change in mass in Sea Carousel may be defined as:

$$\partial M/\partial t = - \delta \, \partial S/\partial x \, A\varepsilon/V \qquad (2)$$

where A is the area over which diffusion takes place (0.012 m^2), V is the volume of Sea Carousel (0.218 m^3), and ε is an efficiency term dependent on the azimuthal velocity ($\varepsilon \propto \bar{U}_y$). Measurements of $\partial M/\partial t$ at different constant azimuthal velocities yield a concentration half-life ($S_{½}$) of 2400 seconds, setting $\varepsilon = \bar{U}_y$ and $\partial S/\partial x$ to $(S_1 - S_0)$, the quotient $(-\delta A/\partial x)$ is derived

$$\partial M = - 3.3 \times 10^{-3}(S_1 - S_o)\bar{U}_y \, \partial t \qquad (3).$$

The loss of mass through dispersion, calculated using equation 3, is added to measured annulus mass (SV) to derive a measure of the total mass, where V is the annulus volume (0.218 m^3).

5.0 DATA COLLECTION

Good results were obtained from 6 stations listed in Table 5.1. Results were obtained from water depths of 11.6 m to 23.5 m. Video results (VHS) were obtained at all stations, while high resolution Sony Hi8 was obtained from all but one station.

STATION	LATITUDE	LONGITUDE	DEPTH (m)	TIME (mins)	SUB-SAMPLE	VIDEO 1/2
SJ1	45 12.60	66 00.95	11.6	51	4	1/2
SJ2	45 12.84	66 01.10	18.9	102	8	1/2
SJ3	45 12.61	66 01.59	19.2	72	7	1/2
SJ4	45 12.28	66 01.07	22.9	127	1	2
SJ6	45 12.87	66 02.19	16.8	79	--	1/2
SJ7	45 12.50	66 01.36	23.5	55	--	1/2

Table 5.1 A summary of the Sea Carousel deployments undertaken aboard MV Irish Lass (Video

1 - Sony Hi8; Video 2 - VHS camera (low resolution)).

6.0 RESULTS

6.1 Sensor Calibration

The calibration of the two internal OBS sensors was undertaken by sampling the sediment/water slurry by pumping from a sample port in the side of Sea Carousel. Samples were collected at each station where this was possible. No samples were obtained at stations SJ6 and SJ7 because of the strong (1.5 - 2.0 m/s) currents.

Sediment concentration was determined by vacuum filtering a known volume of water through 0.45 micron pore diameter Nuclepore filters. The filtered samples yielded a strong correlation with the OBS voltage detected at the time of pump sampling. The correlations for the two internals sensors are as follows:

$$SSC_{OBS1} = 4.467OBS1_{voltage} - 966 \quad (4)$$

$$SSC_{OBS3} = 3.493OBS3_{voltage} + 9 \quad (5)$$

SAMPLE	TIME (GMT)	SSC (mg/L)	OBS1	OBS3
1/1	1404	28.6	220	-2
1/2	1413	32.2	219	-3
1/3	1421	25.4	218	-4
1/4	1430	21.8	217	-4
2/1	1619	25.2	--	--

SAMPLE	TIME (GMT)	SSC (mg/L)	OBS1	OBS3
2/3	1651	152.4	260	36
2/4	1703	294.8	280	53
2/5	1710	313.5	290	60
2/6	1715	383.4	285	55
2/7	1721	209.4	250	50
2/8	1727	154.8	235	48
3/1	1924	530.6	460	360
3/2	1934	2238	840	920
3/3	1940	6396	1280	1400
3/4	1947	4982	1550	1600
3/5	1953	780.5	1600	1750
3/6	2000	906.5	1650	1780
3/7	2009	1039	1730	1900
4/1	2159	770.7	340	125

Table 6.1.1 The suspended sediment concentrations derived from filtered samples taken from the Sea Carousel at stations SJ1, SJ2, SJ3 and SJ4, and associated OBS voltages.

6.2 Time-Series of Measurements

The time-series measurements for stations SJ1 to SJ7 are shown in Figures 6.2.1, 6.2.3, 6.2.5, 6.2.8, 6.2.10 and 6.2.13 respectively. Each figure illustrates three sets of data collected during the deployments of the Carousel: (1) azimuthal current speed, vertical current speed and lid rotation, all displayed in m/s; (2) the SSC recorded by each internal OBS sensor, the raw (uncorrected) SSC, and the ambient SSC; and (3) the rate of erosion determined from the rate of change in SSC.

SJ1 shows a high degree of irregularity in the azimuthal current that is diagnostic of a rough seabed and a lack of a complete seal around the base of the Carousel (Figure 6.2.1). Also, the low peak lid speed of 0.55 m/s suggests that a large amount of energy was used in overcoming bottom friction rather than accelerating the flow. SSC values were exclusively less than 70 mg/L and the ambient SSC was equal to the internal; thus no net bed erosion took place. Peaks in the erosion rate (3×10^{-3} kg/m^2/s) at the onset of flow and after a brief period of still-water (when the cable was trapped in the lid) is likely the result of the suspension of organic matter. The friction angle of 90° (Figure 6.2.2) and the lack of a measurable cohesion are diagnostic of a hard seabed, possibly bedrock.

SJ2 also shows a high degree of macroturbulence in the azimuthal current speed, again diagnostic of a rough bottom (gravel/sand). The step-like increase in SSC, however, suggests that bed erosion has taken place (Figure 6.2.3). The ramping of the ambient SSC is diagnostic of serious leakage of the Carousel due to an imperfect seal at the base. The rapid decline of OBS1 and OBS3 are also diagnostic of this. Consequently, the rate of erosion estimates must be treated with caution. The low cohesion or critical erosion threshold of 0.5 Pa is typical of the onset of

transport of non-cohesive fine sand. The high friction angle 87° is also typical of very low effective stresses (Figure 6.2.4).

SJ3 shows a much more ordered and controlled increase in azimuthal current, together with a low signal variance (Figure 6.2.5). The vertical component of flow also shows a low signal variance which indicates low levels of macroturbulence associated with a smooth seabed that is typical of muddy bottoms. Corrected SSC reaches enormously high levels of 30 g/L with associated erosion rates in excess of 1 x 10^{-2} kg/m^2/s. These are amongst the highest rates ever recorded with Sea Carousel and attest to the instability of these deposits. The surface is armoured relative to the subsurface, exhibiting a surface cohesion of 1.0 Pa that decreases in a hyperbolic fashion over 2 mm to zero resistance (fluidized bed) with no friction angle (Figure 6.2.6).

SJ4 shows a bed stability which is intermediate between stations SJ2 and SJ3 (Figure 6.2.8). The current speed variance and SSC are also intermediate. SSC increases to a maximum of *circa* 3 g/L and shows erosion at all velocities with peaks of 2 - 3 x 10^{-3} kg/m^2/s. The station is punctuated by a break in lid rotation brought about by cables being dragged into the lid path by the strong ambient currents. The erosion prior to the break was Type I erosion (benign) whereas the erosion rate after the break was typical of Type II. The cohesion at this station was 1.0 Pa, but again, the bed was in a fluidized state as indicated by the zero friction angle (Figure 6.2.9).

SJ5 was abandoned as it was impossible for the boat to hold anchor due to strong (2 m/s) currents. The Carousel was torn out of its seabed position on four or five occasions before this decision was made.

SJ6 demonstrates a classic stepwise increase in current speed with time that is not so

evident in earlier deployments. The peak speed of *circa* 0.6 m/s is diagnostic of a smooth bed and the suppression of marcrotubulent events (Figure 6.2.10). SSC shows levels second only to those detected at station SJ3 (13 g/L). The early peak in SSC of OBS3 and raw OBS are due to the landing of the Carousel. OBS1 shows a near perfect trend in SSC increasing an Type I fashion for the first half of the experiment, thereafter altering to Type II erosion. Notice the change in erosion rate pattern between Type I and II erosion trends (Figure 6.2.11). The peaks in Type I erosion reach 2 x 10^{-2} kg/m^2/s, but are short-lived (3 minutes). Type II erosion rate appears to be consistently *circa* 1 x 10^{-3} kg/m^2/s. The cohesion at this site is 1.0 Pa and the bed shows a decrease in strength with depth diagnostic of a fluidized bed.

SJ7 shows similar results to station SJ6 (Figure 6.2.13). Again a clear stepwise progression in current speed is evident and low levels of macroturbulence. On the other hand, SSC levels are less than 10% of those seen in station SJ6 reaching only 700 mg/L. The pattern of SSC change and the unaccountable losses are diagnostic of an imperfect seal at the base, caused through lifting the Carousel by the very strong ambient tidal currents (2.5 m/s) during the early stages of the experiment. Erosion rates were much lower that at station SJ6 being *circa* 10^{-3} kg/m^2/s. The seabed at this station shows a normal pattern typical of a steadily consolidating bed; strength increases systematically beneath the mudline. Also, Type Ia, Type Ib and Type II erosion are evident (Figure 6.2.14). Cohesion is 1.0 Pa and the friction angle is 80°.

STATION #	SSC_{MAX} (mg/L)	COHESION (Pa)	FRICTION ANGLE	EROSION TYPE
SJ1	75	> 5	90	--

STATION #	SSC_{MAX} (mg/L)	COHESION (Pa)	FRICTION ANGLE	EROSION TYPE
SJ2	325	0.5	87	--
SJ3	6500	1.0	0	II
SJ4	1600	1.0	0	II
SJ6	2600	1.0	0	II
SJ7	340	1.0	80	Ia,Ib,II

Table 6.2.1 A summary of the results of the six stations occupied during this survey. The stations fall into three broad groups: (1) hard non-erodible substrate (SJ1, SJ2); (2) very soft highly erodible, fluidized substrates (SJ3, SJ4, SJ6); and (3) a consolidated erodible substrate (SJ7).

6.3 Critical Shear Stresses

The critical shear stresses for bed erosion fall into two groups: (1) non-erodible material of strengths above those applied in this study (SJ1, SJ2); and (2) erodible material (SJ3, SJ4, SJ6, SJ7). Results from group 2 show a consistent trend, and are representative of the finer-grained substrates. The almost universal value of 1.0 Pa was found despite large differences in the erosion rate and friction angles. In some cases the strength at the surface was greater than at depth (a negative friction angle; SJ3, SJ4, SJ6) suggestive of a fluidized bed in which the surface has been armoured either biologically or by rheological processes.

6.4 Erosion Rates

The peak erosion rates varied between 7×10^{-4} to 0.01 $kg/m^2/s$. In general, the highest erosion rates were associated with the highest excess bed shear stresses, and a weak

positive correlation is evident in Figure 6.4.1. For the fine-grained sites, station SJ3 showed the greatest erosion rates and station SJ7 showed the lowest. The relatively low erosion rate of the SJ4 data (1.2 Pa) may be associated with biostabilization as discussed in the text.

6.5 Deposition Rates

The two deposition experiments (SJ3 and SJ6) yielded exponentially-decreasing SSC with time (Figures 6.2.7 and 6.2.12). The SSC gradients are defined as follows:

$$SSC(t) = SSC(0).e^{-0.0028t} \quad (6)$$

$$SSC(t) = SSC(0).e^{-0.0020t} \quad (7)$$

Equation 6 is valid for station SJ3 and equation 7 is valid for station SJ6. The mass settling rate of station SJ3 is approximately 30% higher than is that of station SJ6. The concentration half-lives for the two stations are 250 seconds and 350 seconds respectively. These rates are very high and suggest that the material in suspension is composed largely of inorganic silty sediment.

7.0 INTERPRETATIONS

The results from this survey indicate that the seabed material from St John Harbour mouth fall into three major groups: (1) a hard substrate that is resistent to erosion (SJ1, SJ2); (2) a very soft, fluidized substrate that is easily eroded (SJ3, SJ4, SJ6); and (3) a soft consolidated substrate that shows no evidence of fluidization (SJ7). Group 1 was typical of the shoal regions of sand and gravel at dump site B; group 2 was typical of the deeper adjacent areas, presumably the winnowed fines of the dump site B; and group 3 was typical of long-term "normal" sedimentation processes wherein the sediment has time to equilibrate with depth beneath the mudline (SJ7). The nature of the erosion process is highly variable spatially and with depth below the mudline. This is perhaps best seen by comparing station SJ6 and SJ7 that were adjacent to each other at

the reference site. As a consequence, it is difficult to make any predictions about seabed stability without direct measurements.

8.0 RECOMMENDATIONS

The operating conditions for this study were far from optimum due to the extremely strong surface currents. These currents are associated with the spring freshet from the St John River. Future surveys should attempt to miss this period of time.

The dump site B material appeared to have been winnowed since it was dumped in 1992. In order to monitor the evolution of such dumped material, its stability should be monitored immediately after dumping, and thereafter at intervals to determine the rate of armouring. The stability should be referenced to a pre-dump stability survey.

The variability in results between SJ6 and SJ7 attests to the complexity in the depositional history and surficial geology of the region. Seabed stability tests should be carried out to define this variability.

The anchoring capacity of the boat used in this study was insufficient for the present purposes. In future two forward anchors and one stern anchor should be used to moor the boat.

9.0 CONCLUSIONS

Six stations were successfully occupied during this survey: 2 stations on dump site B (SJ1, SJ2), two adjacent to the dump site in deeper water (SJ3, SJ4) and two at a reference site inside St John Harbour (SJ6, SJ7). Three trends were evident in these stations: (1) an armoured seabed resistent to erosion (SJ1, SJ2); (2) a very soft fluidized seabed with an extremely high erosion rate (SJ3, SJ4, SJ6); and (3) a seabed exhibiting a consolidation profile and intermediate erosion rates (SJ7). Stability was inversely related to water depth; the greater the water depth the lower

the stability.

The dump site comprises trend (1) and appears to be composed of gravel, sand and possibly bedrock. It was resistent to erosion by the Carousel. It appears that any material dumped in 1992 has already become winnowed, dispersed and armoured.

The winnowed material adjacent to the dump site comprises trend (2) and appears to have become deposited rapidly. Here it forms a fluidized deposit that nevertheless possesses a yield resistance of 1.0 Pa at its surface. This strength is found only in the topmost 2 mm and is considered to be the result of biostabilization possibly due to a highly productive diatom film (T. Sutherland, pers. comm.). The potential rate of erosion of this material is as high as has ever been observed with Sea Carousel. The transition from bed erosion to bed deposition was found between water depths of 12 and 19 m. Above 12 m the seabed was strongly scoured; below 19 m the bed was largely one of sedimentation.

The reference sites showed a great degree of variability; one being a fluidized bed, the other being consolidated. The cohesion of these sites was similar to that for the winnowed material, however the rates of erosion were much less.

10.0 LIMITATIONS

The results of this study comprise six sites only. Consequently, little can be stated regarding general trends of dump site stability. The results obtained must be considered as preliminary at best. The high currents had a significant impact on the operation. Many disruptions were the result of cables being dragged and jammed in the lid, the lifting of the Carousel off the seabed by fluid drag, and by ship losses of anchor. These may be overcome by adding more weight to the Carousel and by stream-lining the mooring arrangement.

The correction for dispersion of sediment out of the Carousel is valid only if the base is fully sealed. This was not the case for stations SJ1, SJ2 and SJ7. Consequently, unknown losses of eroded sediment must be expected. The results from these stations must, therefore, be considered minimum values.

The frequent disruptions in the experiments due to lid stoppage or dragging has a significant, though largely unknown influence on the seabed erodibility. These disruptions must be considered when interpreting these results.

11.0 REFERENCES

Burt, T.N. 1984. The Carousel: commissioning of a circular flume for sediment transport research. Hydraulic Research Limited Report SR 33.

Downing, J.P. and Beach, R.A. 1989. Laboratory apparatus for calibrating optical suspended solids sensors. Marine Geology 86: 243 - 249.

Hydraulics Research Limited, 1987. Deposition of cohesive sediments in an annular flume. Unpublished Internal Report: 5p.

Postma, H. 1967. Sediment transport and sedimentation in the estuarine environment. in Lauff, G.M. (ed), Estuaries. Publ. American Association for the Advancement of Science, No. 83: 158-179.

Shames, I. 1962. Mechanics of Fluids. Publ. McGraw-Hill Book Company,New York: 555p.

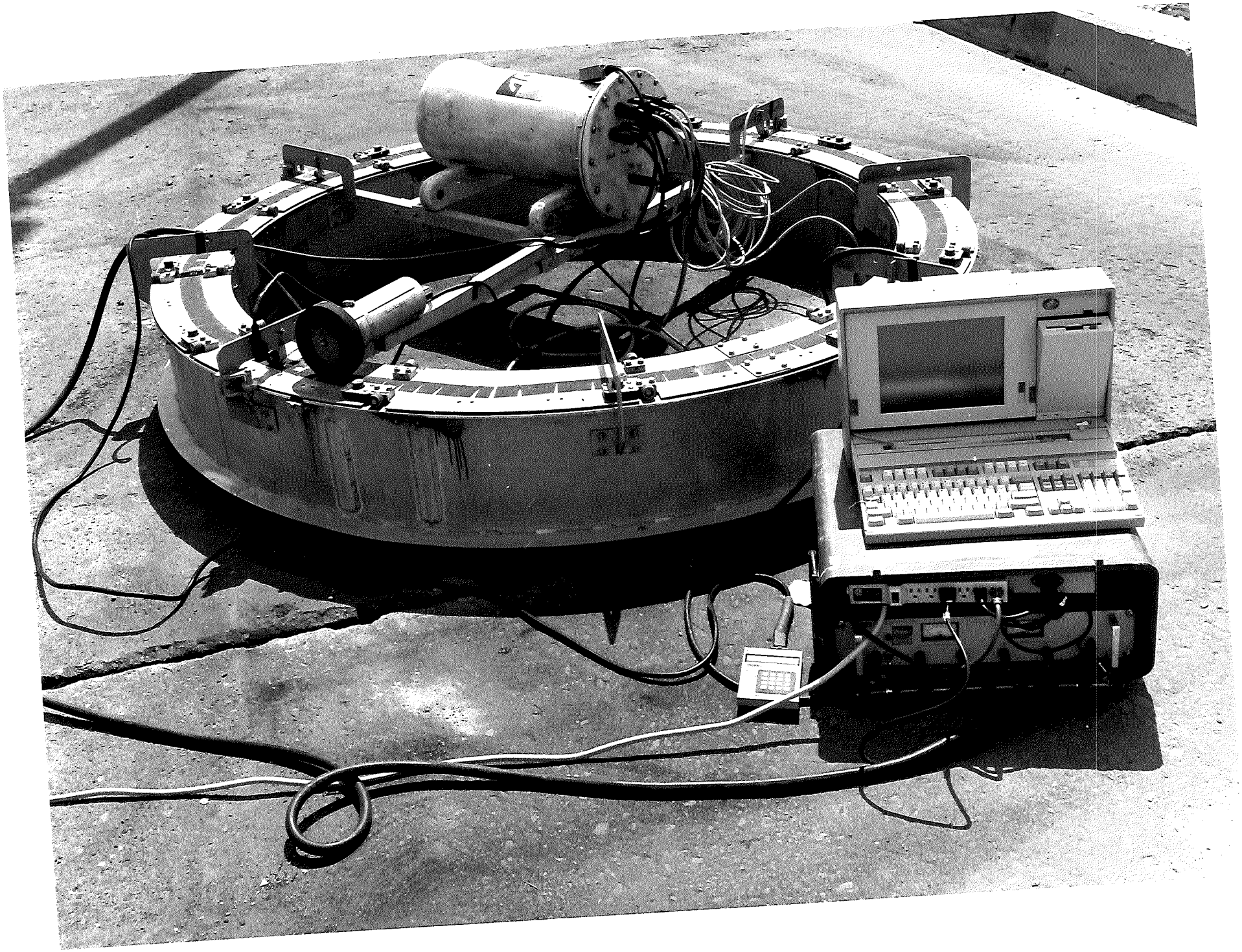

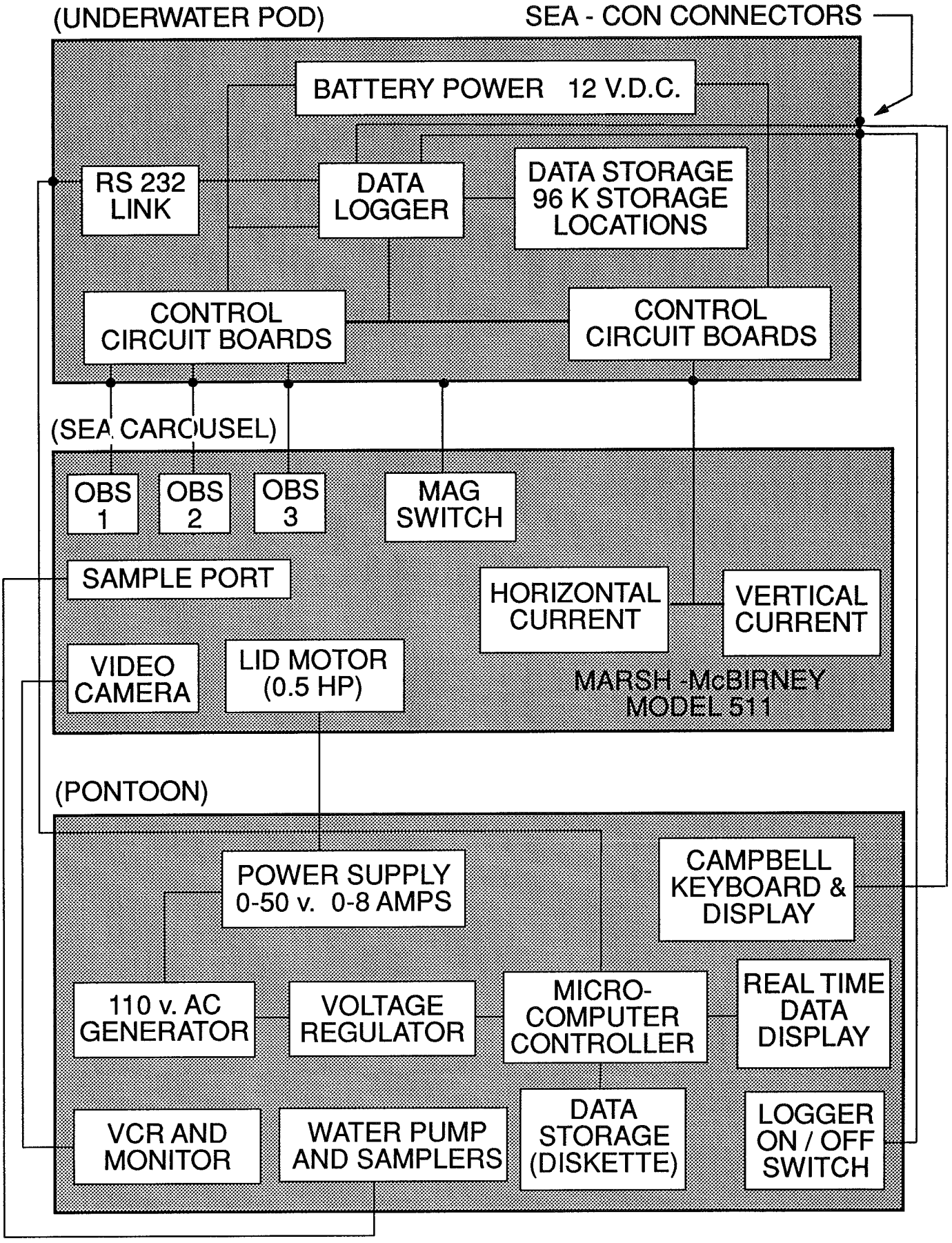
(UNDERWATER POD)
SEA - CON CONNECTORS
BATTERY POWER 12 V.D.C.
RS 232 LINK
DATA LOGGER
DATA STORAGE 96 K STORAGE LOCATIONS
CONTROL CIRCUIT BOARDS
CONTROL CIRCUIT BOARDS
(SEA CARCUSEL)
OBS 1
OBS 2
OBS 3
MAG SWITCH
SAMPLE PORT
HORIZONTAL CURRENT
VERTICAL CURRENT
VIDEO CAMERA
LID MOTOR (0.5 HP)
MARSH -McBIRNEY MODEL 511
(PONTOON)
POWER SUPPLY 0-50 v. 0-8 AMPS
CAMPBELL KEYBOARD & DISPLAY
110 v. AC GENERATOR
VOLTAGE REGULATOR
MICRO-COMPUTER CONTROLLER
REAL TIME DATA DISPLAY
VCR AND MONITOR
WATER PUMP AND SAMPLERS
DATA STORAGE (DISKETTE)
LOGGER ON / OFF SWITCH

FIGURE 4.2

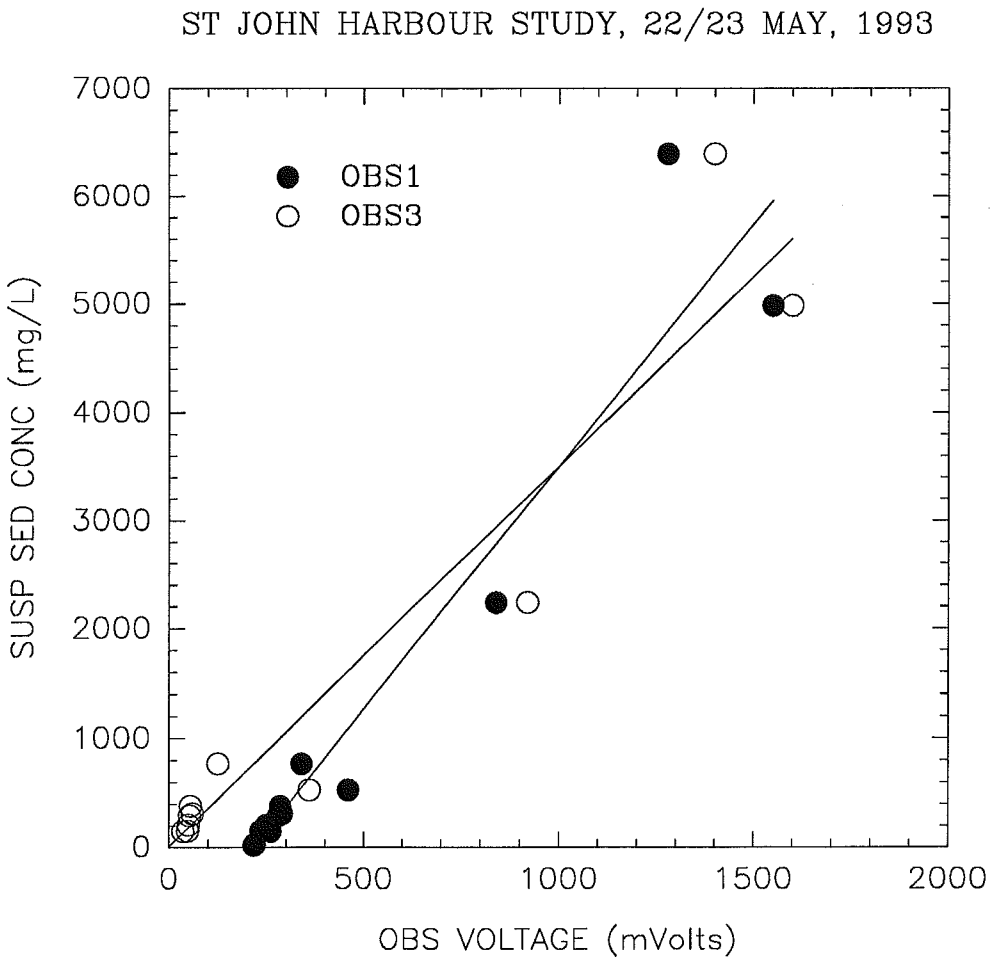
ST JOHN HARBOUR STUDY, 22/23 MAY, 1993
OBS1
OBS3
SUSP SED CONC (mg/L)
OBS VOLTAGE (mVolts)
0
1000
2000
3000
4000
5000
6000
7000
0
500
1000
1500
2000

FIGURE 6.1.1

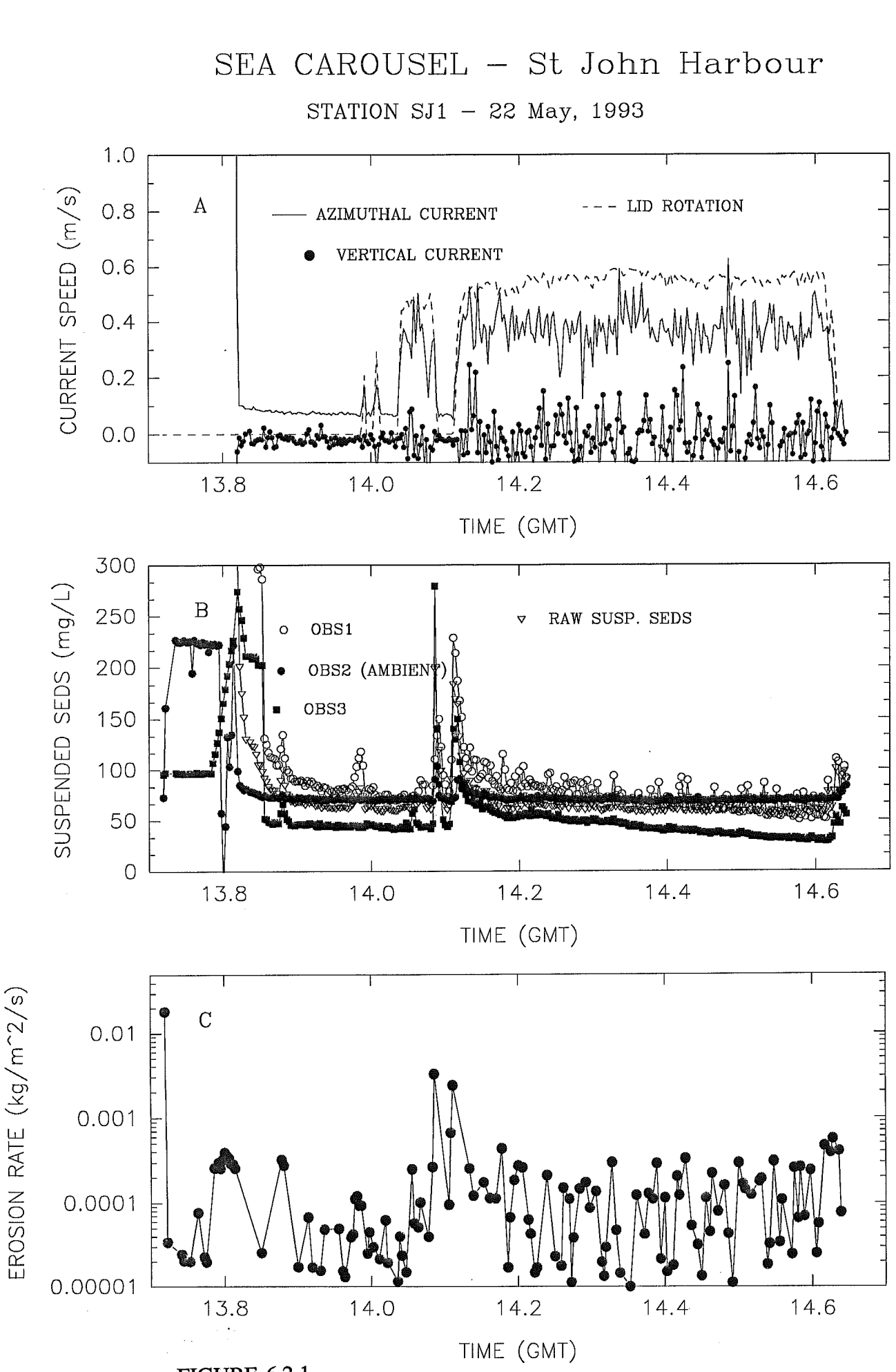
SEA CAROUSEL – St John Harbour
STATION SJ1 – 22 May, 1993
A
AZIMUTHAL CURRENT
LID ROTATION
VERTICAL CURRENT
CURRENT SPEED (m/s)
1.0
0.8
0.6
0.4
0.2
0.0
13.8
14.0
14.2
14.4
14.6
TIME (GMT)
B
OBS1
OBS2 (AMBIENT)
OBS3
RAW SUSP. SEDS
SUSPENDED SEDS (mg/L)
300
250
200
150
100
50
0
13.8
14.0
14.2
14.4
14.6
TIME (GMT)
C
EROSION RATE (kg/m^2/s)
0.01
0.001
0.0001
0.00001
13.8
14.0
14.2
14.4
14.6
TIME (GMT)

FIGURE 6.2.1

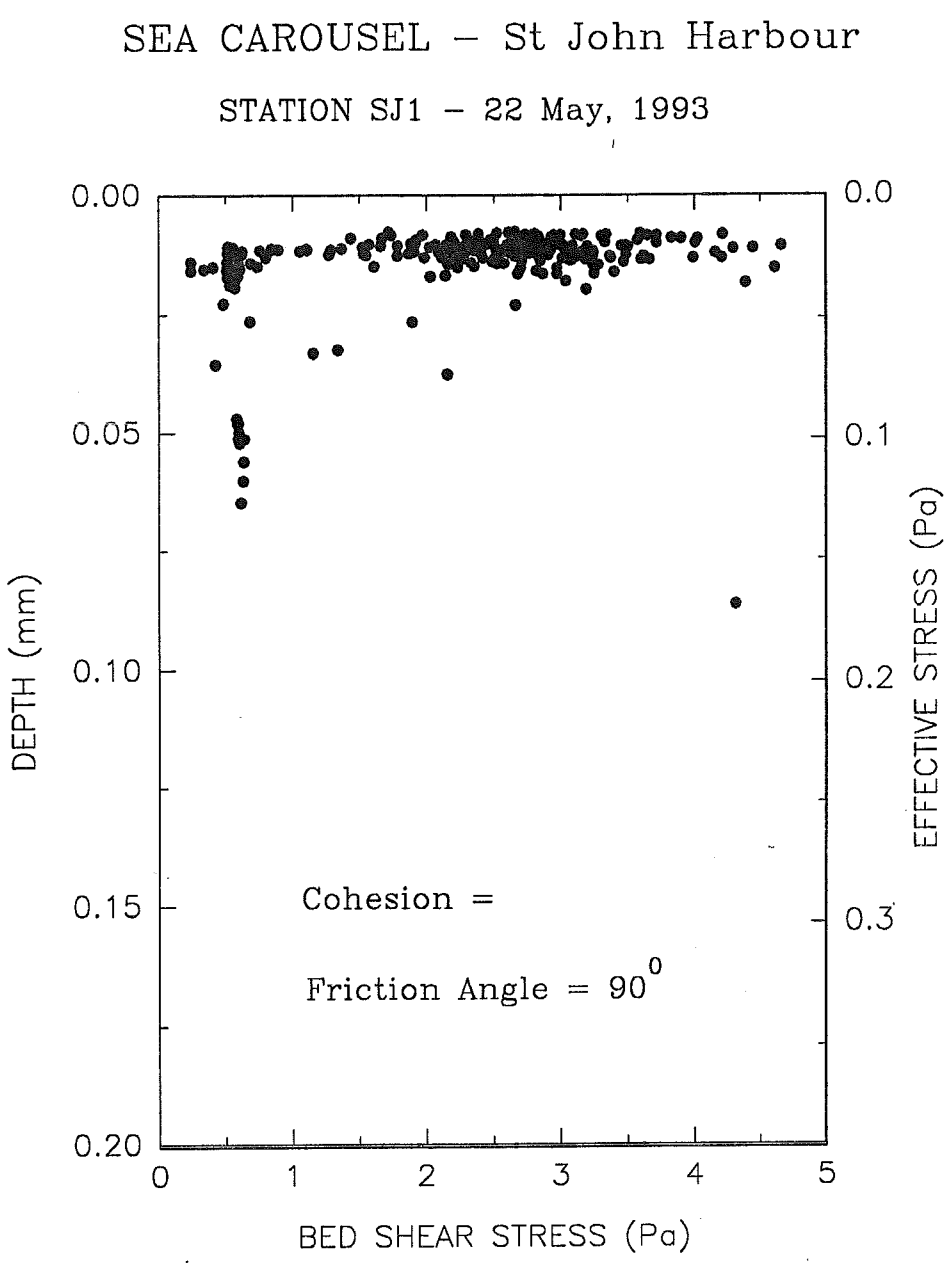
SEA CAROUSEL – St John Harbour
STATION SJ1 – 22 May, 1993
0.00
0.05
0.10
0.15
0.20
DEPTH (mm)
0.0
0.1
0.2
0.3
EFFECTIVE STRESS (Pa)
Cohesion =
Friction Angle = 90^0
0
1
2
3
4
5
BED SHEAR STRESS (Pa)

FIGURE 6.2.2

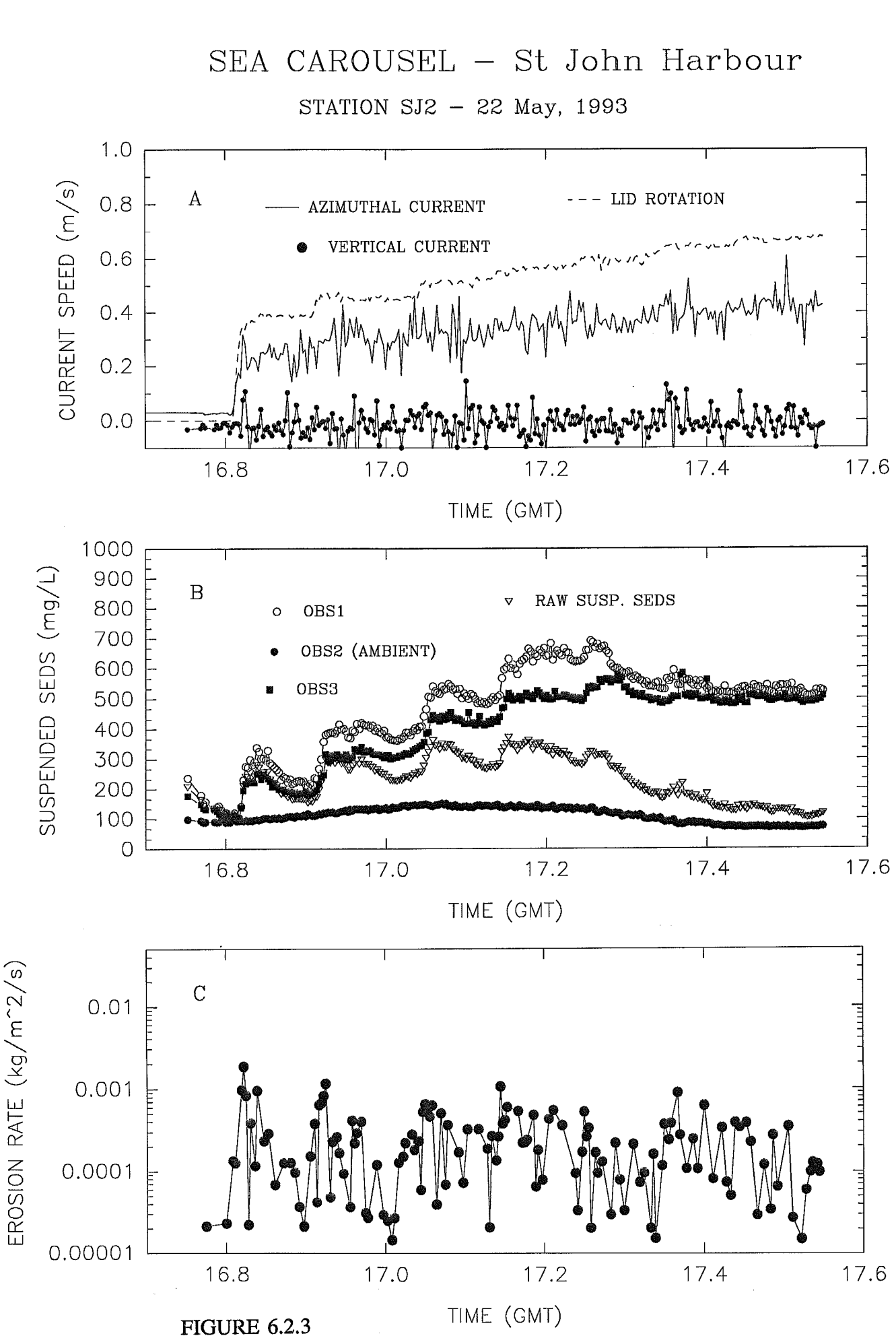
SEA CAROUSEL – St John Harbour
STATION SJ2 – 22 May, 1993
A
AZIMUTHAL CURRENT
LID ROTATION
VERTICAL CURRENT
CURRENT SPEED (m/s)
1.0
0.8
0.6
0.4
0.2
0.0
16.8
17.0
17.2
17.4
17.6
TIME (GMT)
B
OBS1
RAW SUSP. SEDS
OBS2 (AMBIENT)
OBS3
SUSPENDED SEDS (mg/L)
1000
900
800
700
600
500
400
300
200
100
0
16.8
17.0
17.2
17.4
17.6
TIME (GMT)
C
EROSION RATE (kg/m^2/s)
0.01
0.001
0.0001
0.00001
16.8
17.0
17.2
17.4
17.6
TIME (GMT)

FIGURE 6.2.3

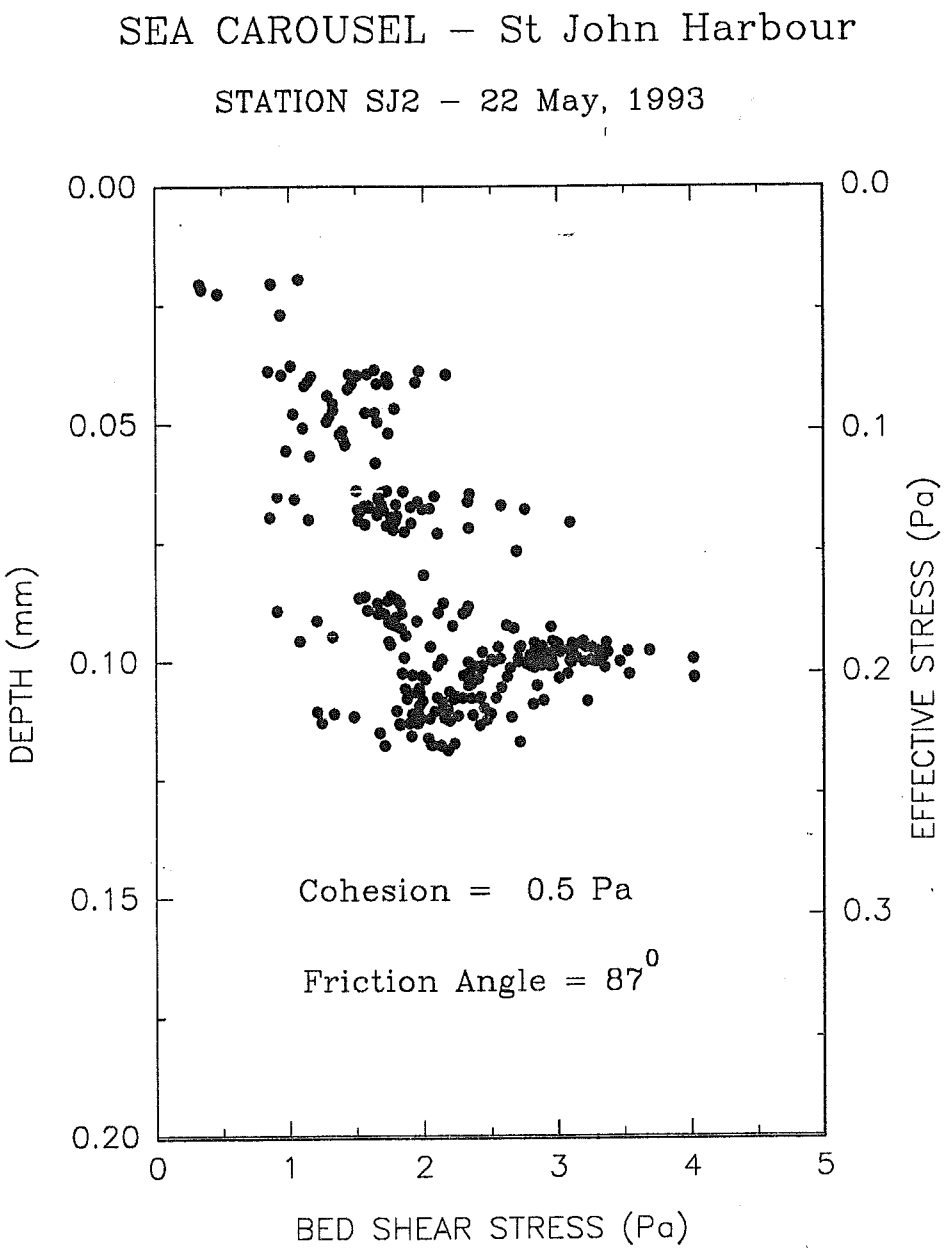
SEA CAROUSEL – St John Harbour
STATION SJ2 – 22 May, 1993
0.00
0.05
0.10
0.15
0.20
DEPTH (mm)
0.0
0.1
0.2
0.3
EFFECTIVE STRESS (Pa)
Cohesion = 0.5 Pa
Friction Angle = 87°
0
1
2
3
4
5
BED SHEAR STRESS (Pa)

FIGURE 6.2.4

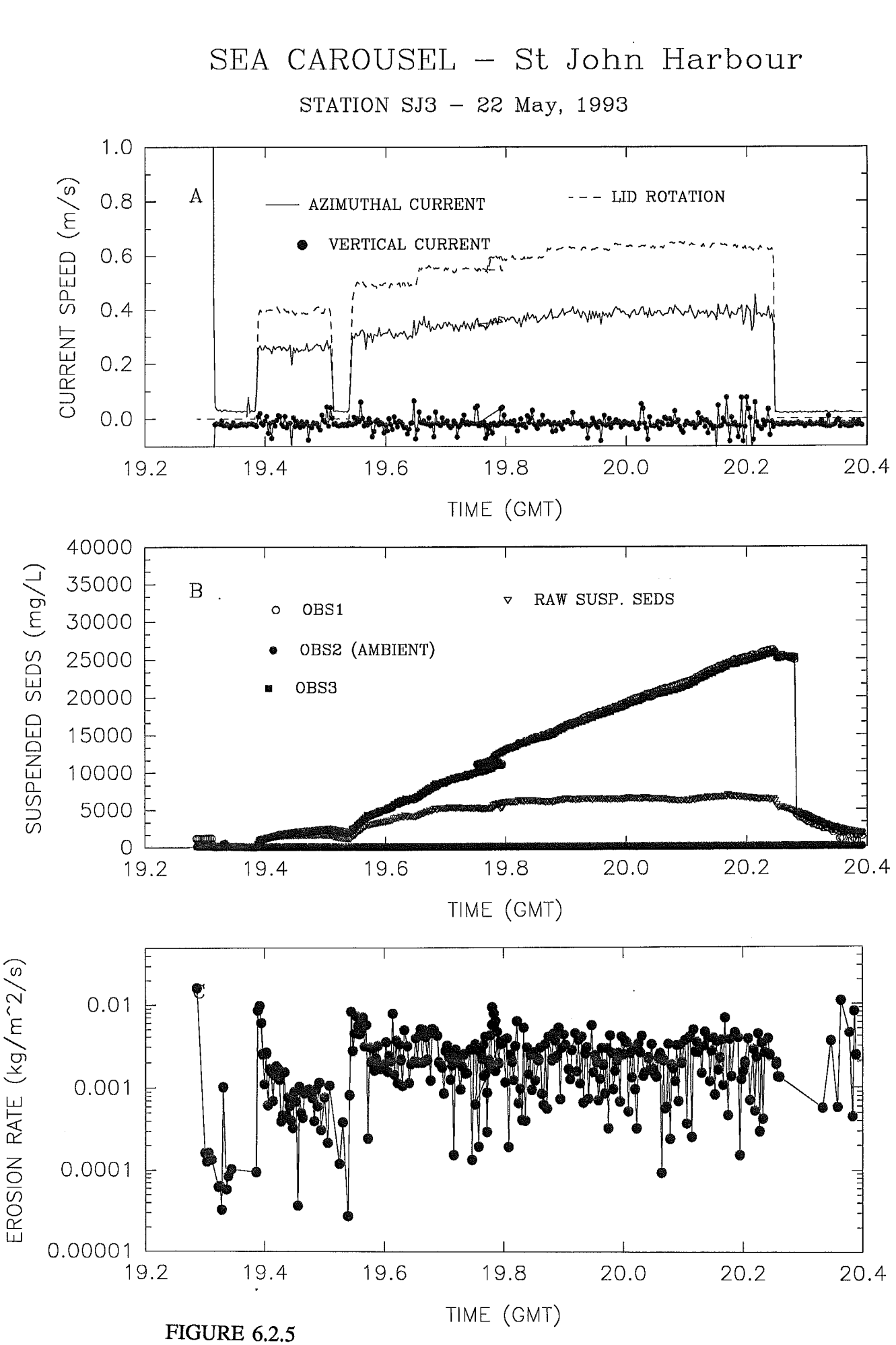
SEA CAROUSEL – St John Harbour
STATION SJ3 – 22 May, 1993
A
AZIMUTHAL CURRENT
LID ROTATION
VERTICAL CURRENT
CURRENT SPEED (m/s)
1.0
0.8
0.6
0.4
0.2
0.0
19.2
19.4
19.6
19.8
20.0
20.2
20.4
TIME (GMT)
B
OBS1
OBS2 (AMBIENT)
OBS3
RAW SUSP. SEDS
SUSPENDED SEDS (mg/L)
40000
35000
30000
25000
20000
15000
10000
5000
0
TIME (GMT)
EROSION RATE (kg/m^2/s)
0.01
0.001
0.0001
0.00001
TIME (GMT)

FIGURE 6.2.5

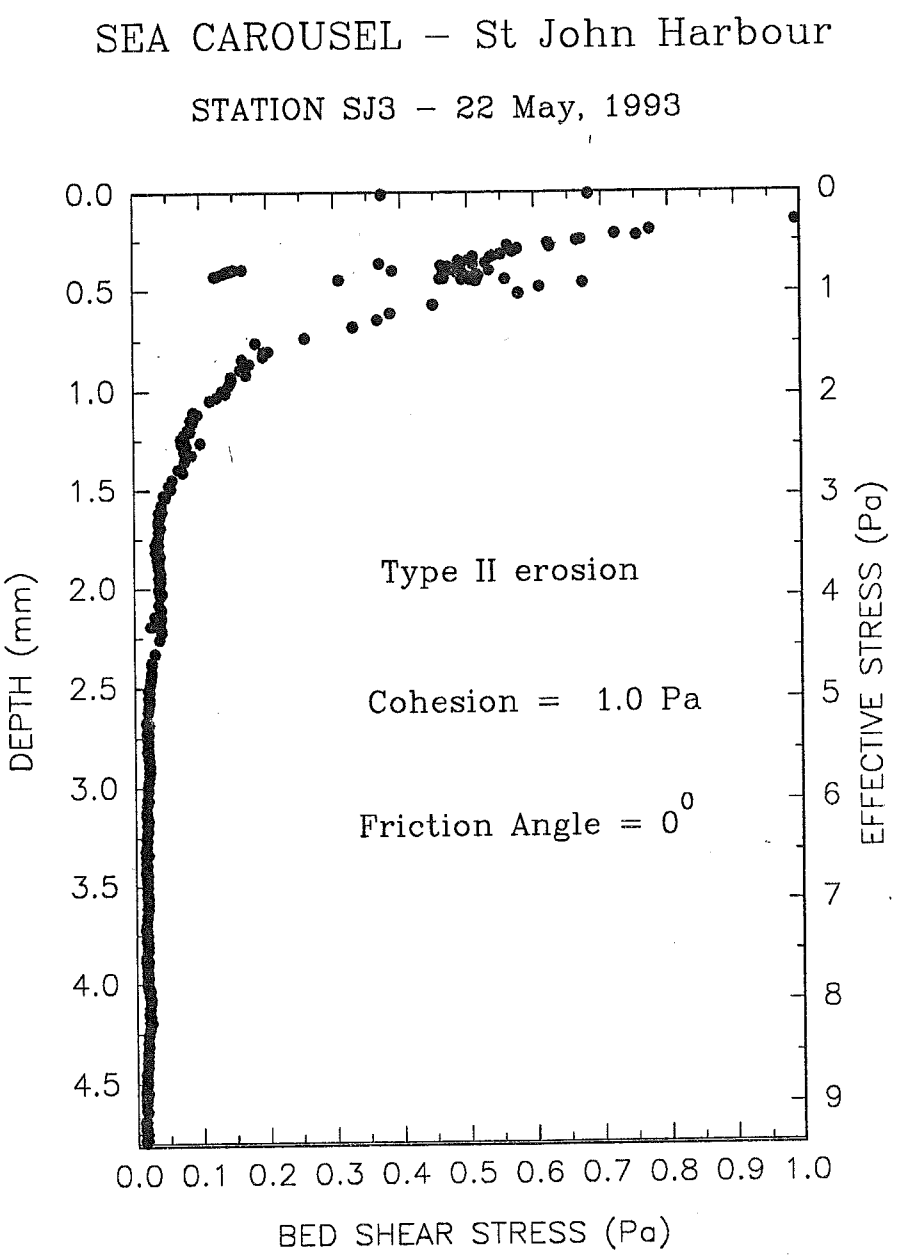
SEA CAROUSEL – St John Harbour
STATION SJ3 – 22 May, 1993
DEPTH (mm)
0.0
0.5
1.0
1.5
2.0
2.5
3.0
3.5
4.0
4.5
EFFECTIVE STRESS (Pa)
0
1
2
3
4
5
6
7
8
9
Type II erosion
Cohesion = 1.0 Pa
Friction Angle = 0°
0.0 0.1 0.2 0.3 0.4 0.5 0.6 0.7 0.8 0.9 1.0
BED SHEAR STRESS (Pa)

FIGURE 6.2.6

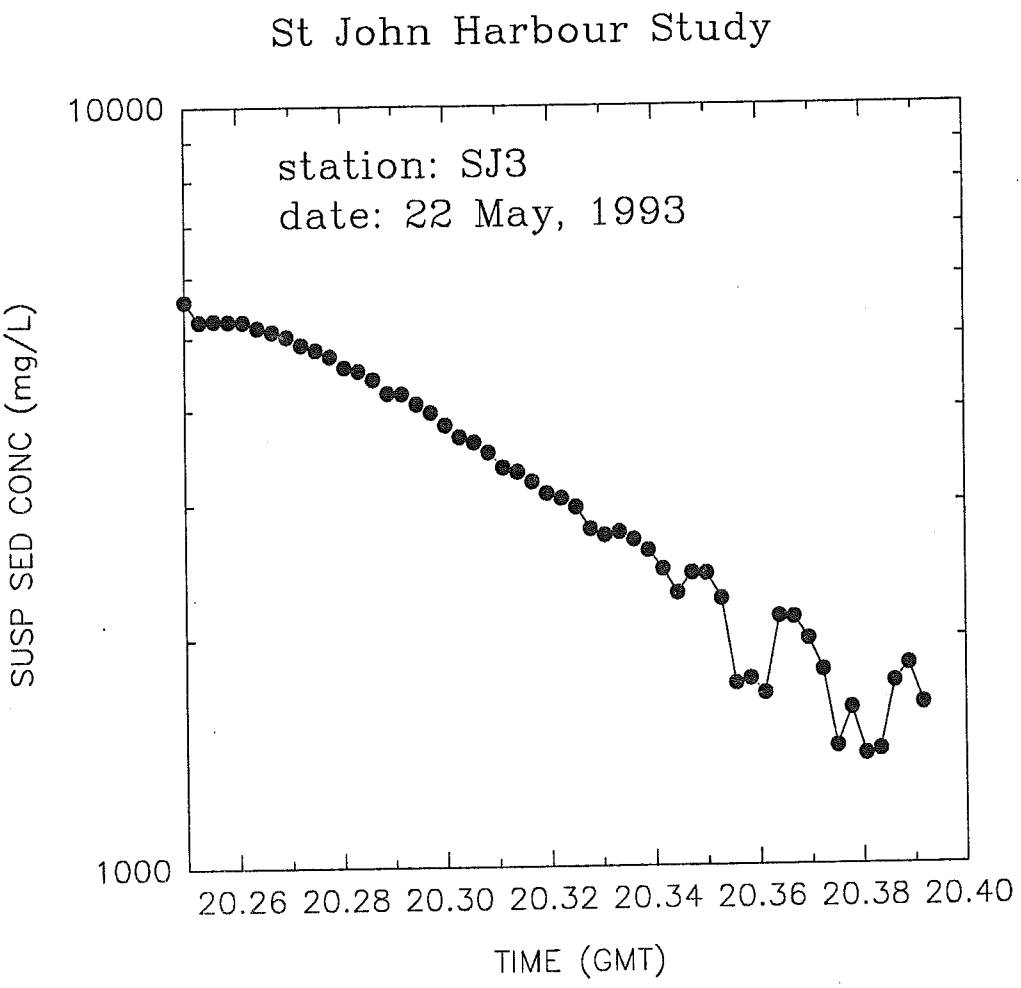
St John Harbour Study
station: SJ3
date: 22 May, 1993
10000
1000
SUSP SED CONC (mg/L)
20.26 20.28 20.30 20.32 20.34 20.36 20.38 20.40
TIME (GMT)

FIGURE 6.2.7

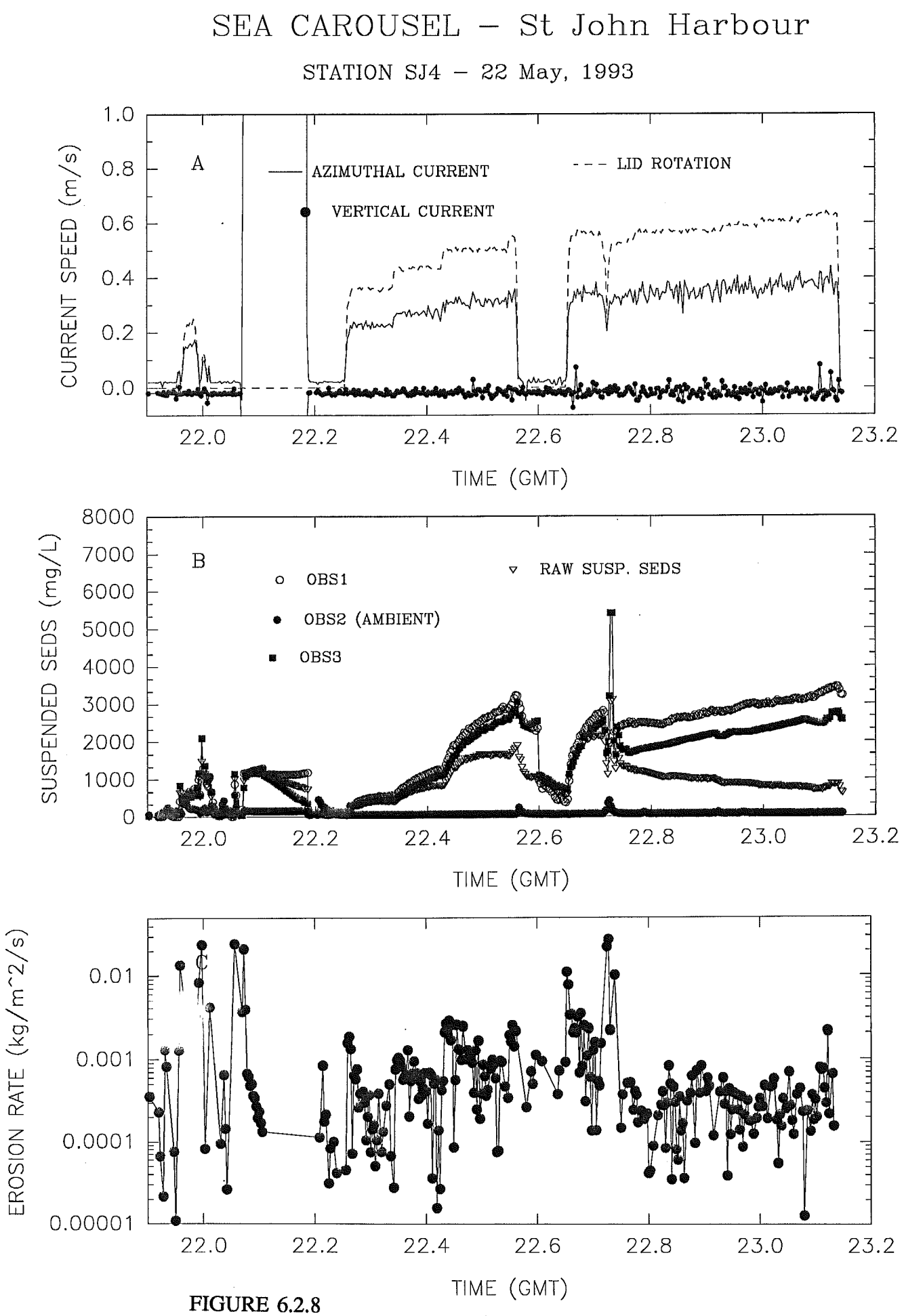
SEA CAROUSEL – St John Harbour
STATION SJ4 – 22 May, 1993
A
AZIMUTHAL CURRENT
VERTICAL CURRENT
LID ROTATION
CURRENT SPEED (m/s)
1.0
0.8
0.6
0.4
0.2
0.0
22.0
22.2
22.4
22.6
22.8
23.0
23.2
TIME (GMT)
B
OBS1
OBS2 (AMBIENT)
OBS3
RAW SUSP. SEDS
SUSPENDED SEDS (mg/L)
8000
7000
6000
5000
4000
3000
2000
1000
0
TIME (GMT)
C
EROSION RATE (kg/m^2/s)
0.01
0.001
0.0001
0.00001
TIME (GMT)

FIGURE 6.2.8

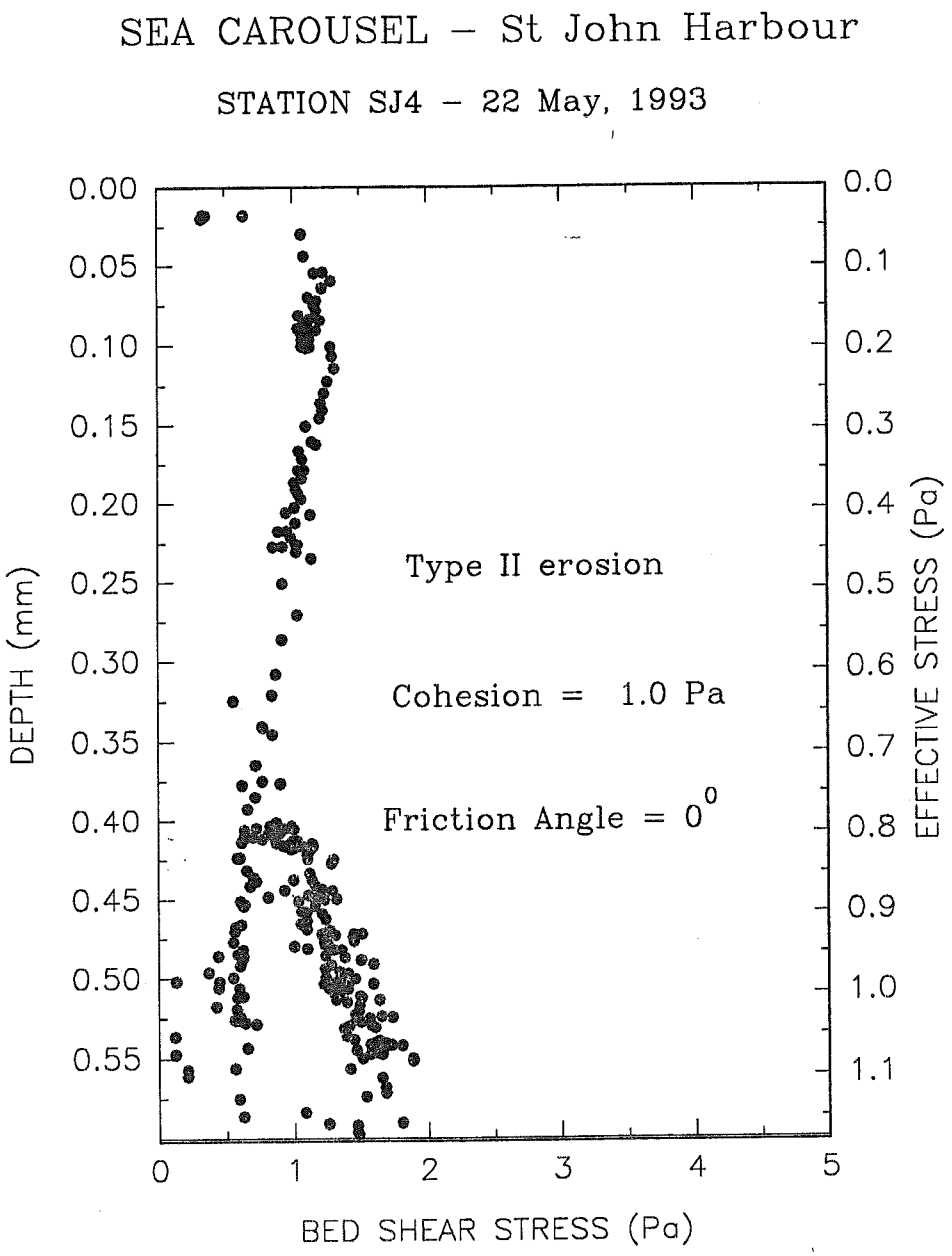
SEA CAROUSEL – St John Harbour
STATION SJ4 – 22 May, 1993
DEPTH (mm)
0.00
0.05
0.10
0.15
0.20
0.25
0.30
0.35
0.40
0.45
0.50
0.55
EFFECTIVE STRESS (Pa)
0.0
0.1
0.2
0.3
0.4
0.5
0.6
0.7
0.8
0.9
1.0
1.1
Type II erosion
Cohesion = 1.0 Pa
Friction Angle = 0°
0
1
2
3
4
5
BED SHEAR STRESS (Pa)

FIGURE 6.2.9

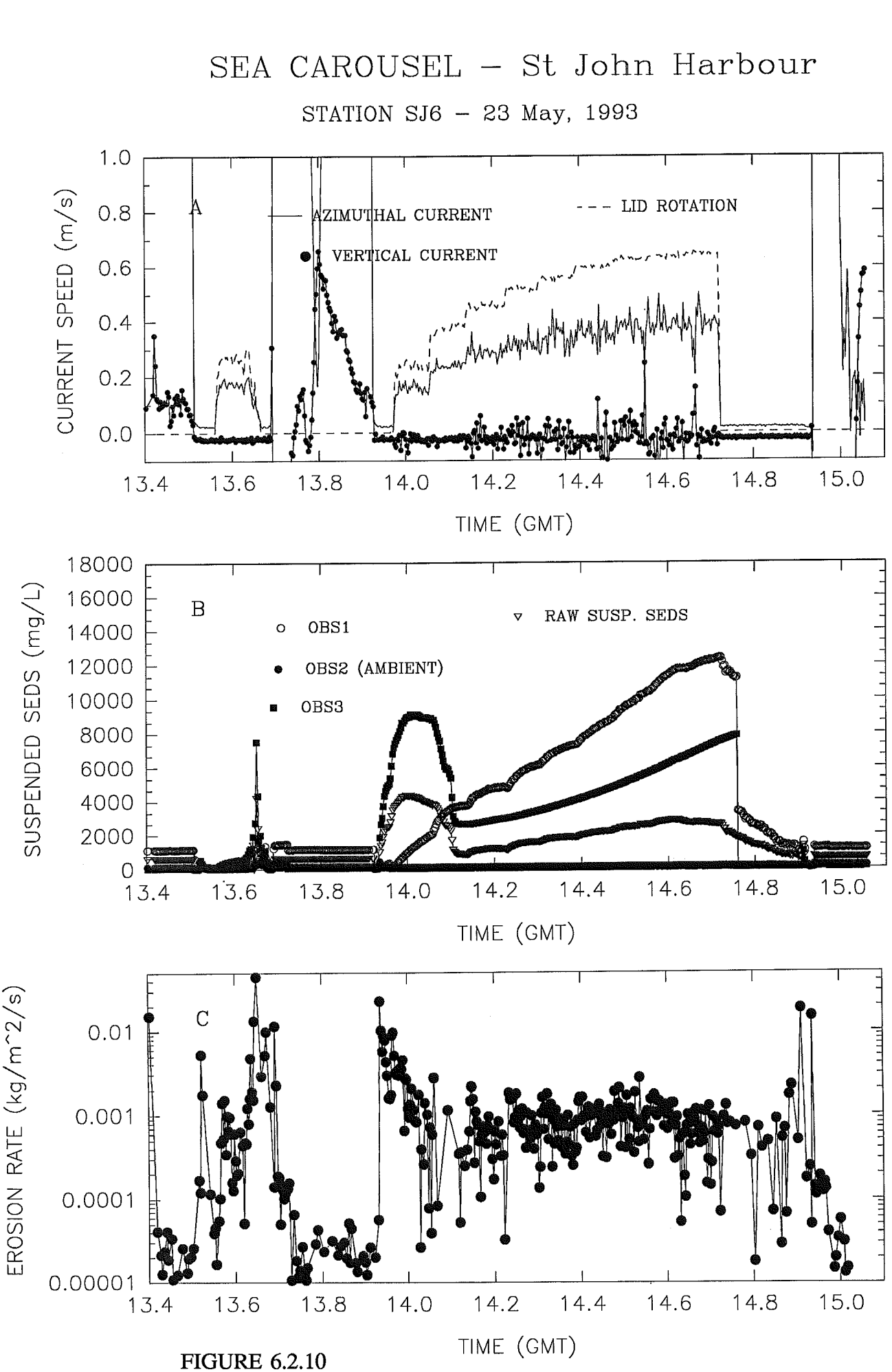
SEA CAROUSEL – St John Harbour
STATION SJ6 – 23 May, 1993
A
AZIMUTHAL CURRENT
VERTICAL CURRENT
LID ROTATION
CURRENT SPEED (m/s)
1.0
0.8
0.6
0.4
0.2
0.0
13.4
13.6
13.8
14.0
14.2
14.4
14.6
14.8
15.0
TIME (GMT)
B
OBS1
OBS2 (AMBIENT)
OBS3
RAW SUSP. SEDS
SUSPENDED SEDS (mg/L)
18000
16000
14000
12000
10000
8000
6000
4000
2000
0
TIME (GMT)
C
EROSION RATE (kg/m^2/s)
0.01
0.001
0.0001
0.00001
TIME (GMT)

FIGURE 6.2.10

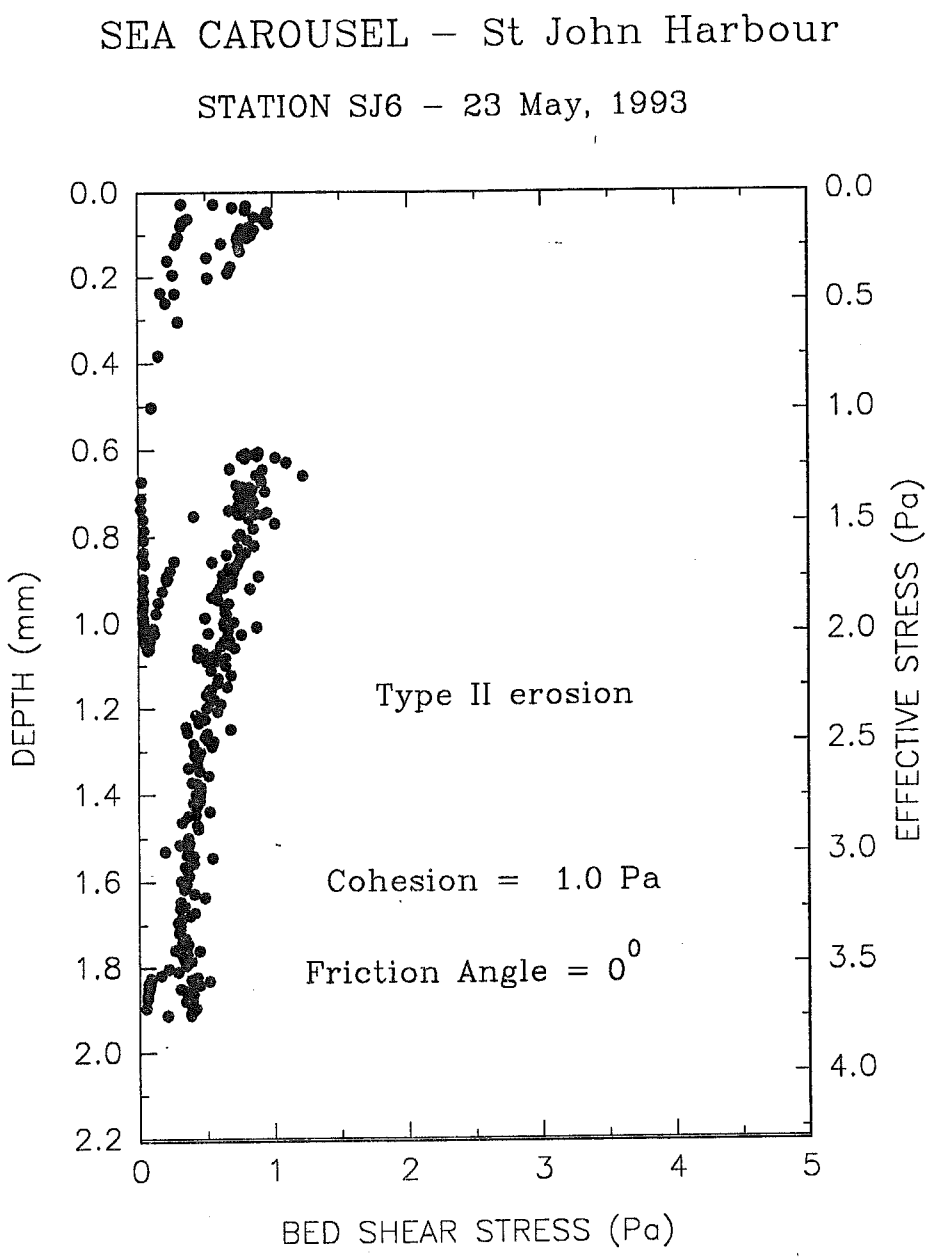
SEA CAROUSEL – St John Harbour
STATION SJ6 – 23 May, 1993
DEPTH (mm)
0.0
0.2
0.4
0.6
0.8
1.0
1.2
1.4
1.6
1.8
2.0
2.2
EFFECTIVE STRESS (Pa)
0.0
0.5
1.0
1.5
2.0
2.5
3.0
3.5
4.0
Type II erosion
Cohesion = 1.0 Pa
Friction Angle = 0^0
0
1
2
3
4
5
BED SHEAR STRESS (Pa)

FIGURE 6.2.11

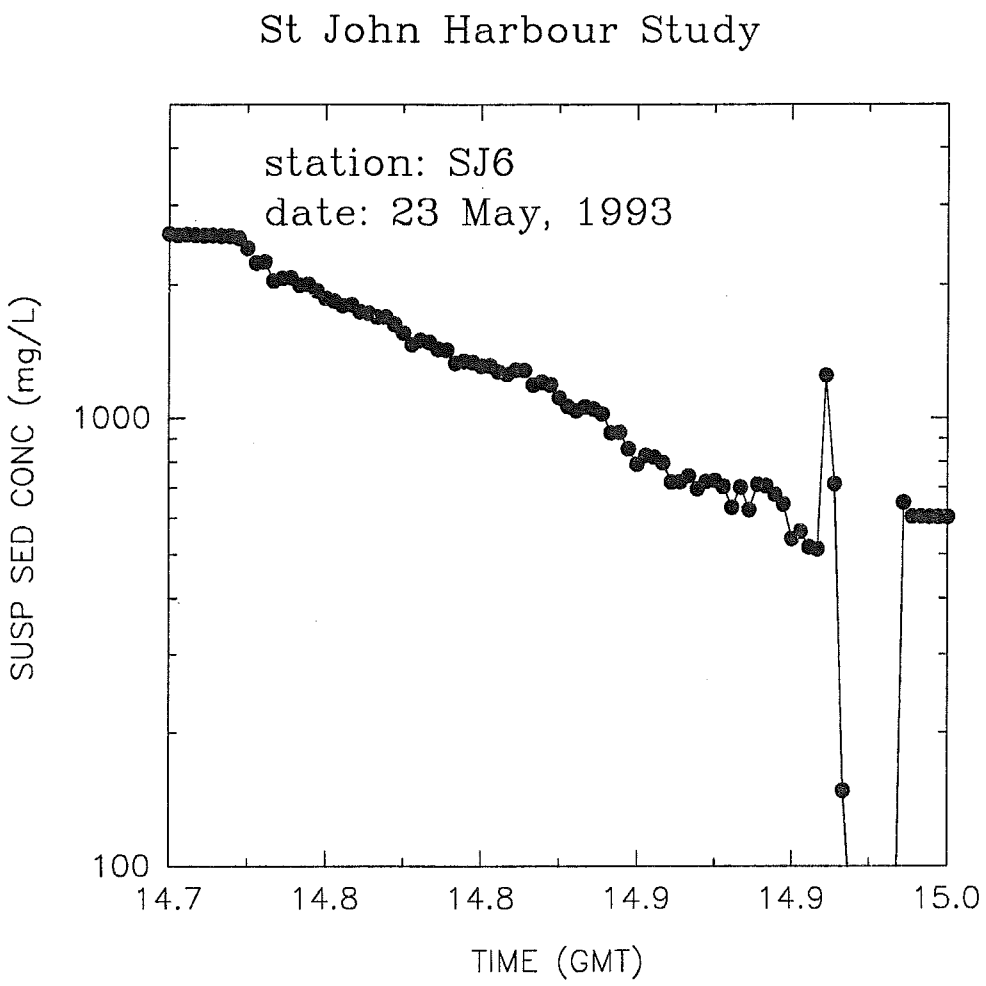
St John Harbour Study
station: SJ6
date: 23 May, 1993
SUSP SED CONC (mg/L)
1000
100
14.7
14.8
14.8
14.9
14.9
15.0
TIME (GMT)

FIGURE 6.2.12

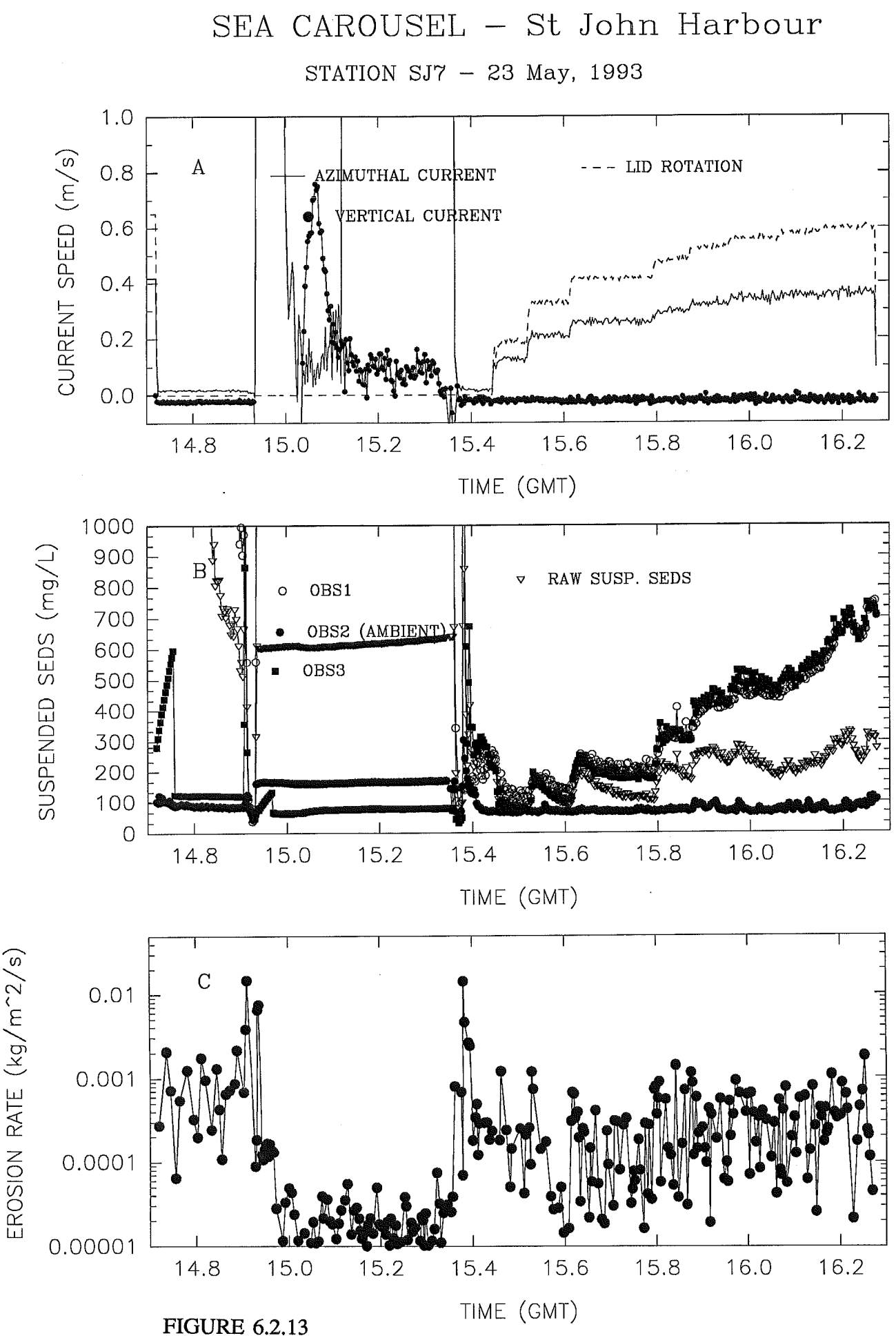
SEA CAROUSEL – St John Harbour
STATION SJ7 – 23 May, 1993
A
AZIMUTHAL CURRENT
VERTICAL CURRENT
LID ROTATION
CURRENT SPEED (m/s)
1.0
0.8
0.6
0.4
0.2
0.0
14.8
15.0
15.2
15.4
15.6
15.8
16.0
16.2
TIME (GMT)
B
OBS1
OBS2 (AMBIENT)
OBS3
RAW SUSP. SEDS
SUSPENDED SEDS (mg/L)
1000
900
800
700
600
500
400
300
200
100
0
TIME (GMT)
C
EROSION RATE (kg/m^2/s)
0.01
0.001
0.0001
0.00001
TIME (GMT)

FIGURE 6.2.13

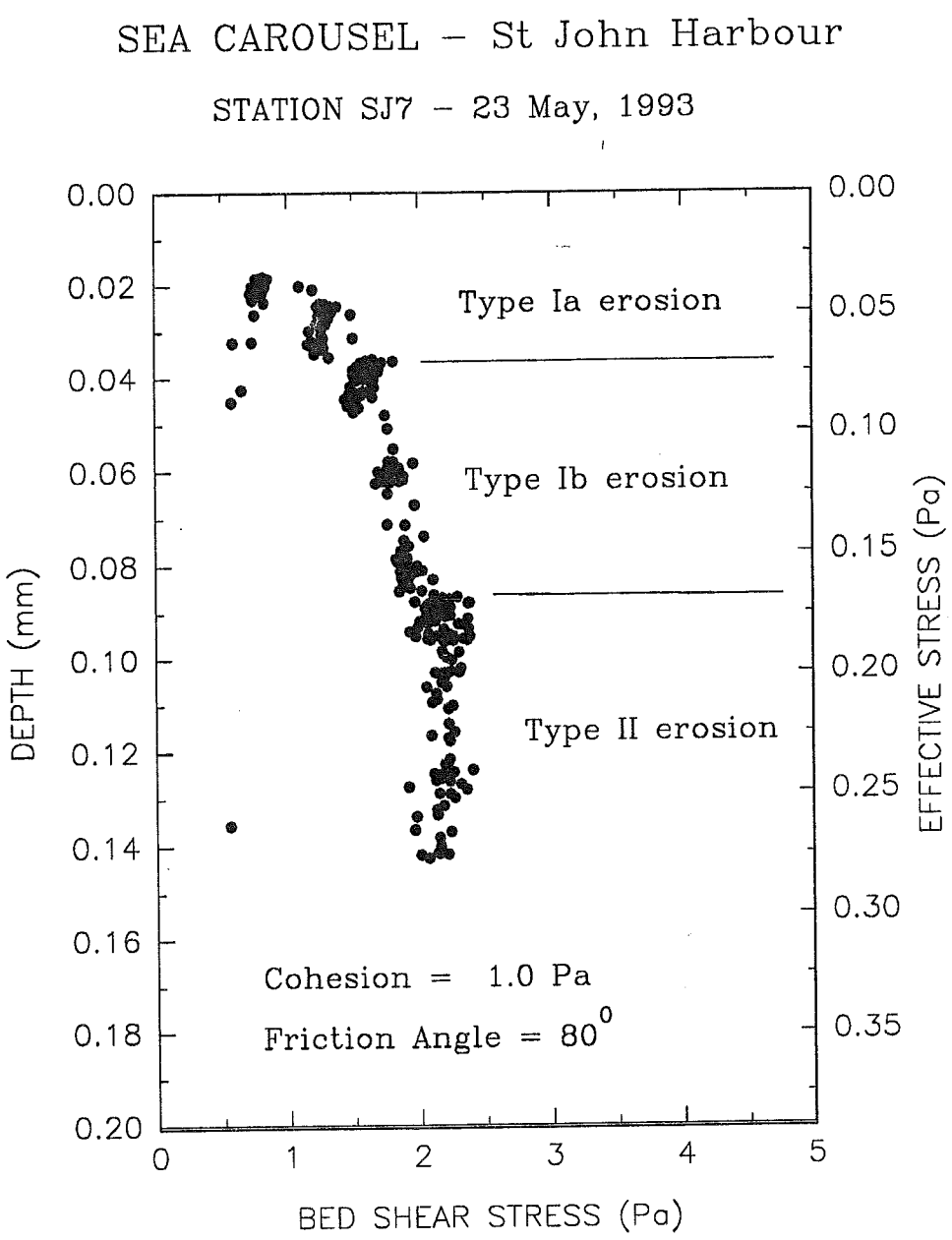
SEA CAROUSEL – St John Harbour
STATION SJ7 – 23 May, 1993
Type Ia erosion
Type Ib erosion
Type II erosion
Cohesion = 1.0 Pa
Friction Angle = 80°
DEPTH (mm)
EFFECTIVE STRESS (Pa)
BED SHEAR STRESS (Pa)
0.00
0.02
0.04
0.06
0.08
0.10
0.12
0.14
0.16
0.18
0.20
0.05
0.10
0.15
0.20
0.25
0.30
0.35
0
1
2
3
4
5

FIGURE 6.2.14

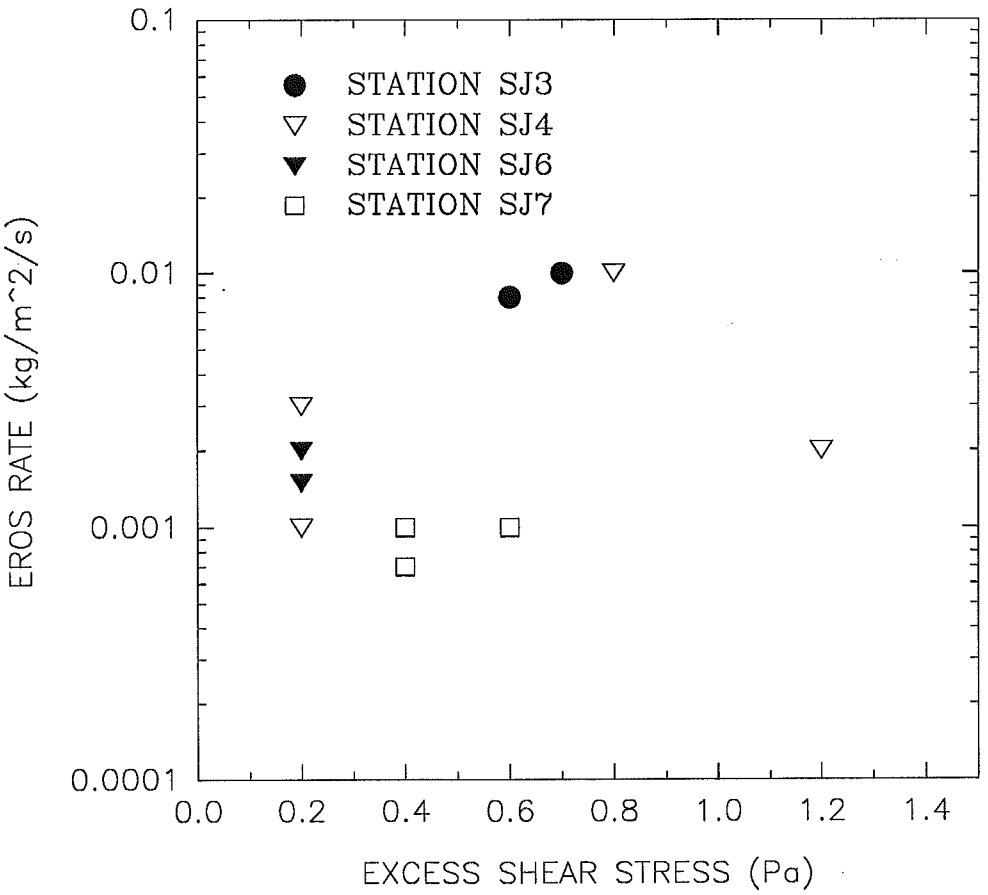
0.1
0.01
0.001
0.0001
EROS RATE (kg/m^2/s)
STATION SJ3
STATION SJ4
STATION SJ6
STATION SJ7
0.0
0.2
0.4
0.6
0.8
1.0
1.2
1.4
EXCESS SHEAR STRESS (Pa)

FIGURE 6.4.1